Experimental Aerodynamics of a Rotor Entry Vehicle

ALAN D. LEVIN* AND RONALD C. SMITH†
NASA Ames Research Center, Moffett Field, Calif.

An unpowered rotor entry vehicle model has been tested at Mach numbers 0.10 to 3.54 at angles of attack from 15° to 90°. The tests included variations of blade collective and cyclic pitch angles. A summary of the autorotative equilibrium rotor speed, forces, and moments is presented. The results indicate that adding the rotor to the capsule improved vehicle performance throughout most of the Mach number range. Maximum lift drag ratio was substantially improved at low Mach numbers. Large pitching moments were produced by the rotor, requiring the use of flaps for longitudinal trim. Control phasing was unusual compared to the predicted response of an "ideal rotor" but did not change grossly with forward flight speed.

Nomenclature

A_c = capsule area, $\pi d^2/4$
b = number of blades
C_{D_r} = rotor drag coefficient, rotor drag/$q_\infty \pi R^2$
$C_{D_{\alpha=90°}}$ = vehicle drag coefficient at $\alpha = 90°$, vehicle drag/$q_\infty A_c$
C_L = lift coefficient, lift/$q_\infty A_c$ (see Fig. 1)
C_l = body-axis rolling moment coefficient, rolling moment/$q_\infty A_c d$
C_{l_θ} = roll control power, $(\partial C_l/\partial \Theta_{1_s})$ and $(\partial C_l/\partial \Theta_{1_c})$; evaluated at 0° cyclic pitch
C_m = pitching moment coefficient, pitching moment/$q_\infty A_c d$
C_{m_θ} = pitch control power, $(\partial C_m/\partial \Theta_{1_s})$ and $(\partial C_m/\partial \Theta_{1_c})$; evaluated at 0° cyclic pitch
c = blade chord
d = capsule diameter
L/D = lift-drag ratio
M_∞ = freestream Mach number
q_∞ = freestream dynamic pressure
R = rotor radius
R_{LE} = leading-edge radius of blade airfoil section
V_∞ = freestream velocity
α = angle of attack
δ_f = flap deflection angle
θ_0 = collective blade pitch angle
θ_{1_s} = longitudinal cyclic blade pitch angle
θ_{1_c} = lateral cyclic blade pitch angle
σ = rotor solidity, $bc/\pi R$
Ψ = blade azimuth angle
Ω = rotational speed

Introduction

AN unpowered depolyable rotor for space vehicle recovery offers several advantages over other recovery techniques, some of which are unique to rotors. The unpowered rotor has the potential of providing initial stabilization, controlled deceleration, lift for maneuvering, and stored energy for land recovery. In addition, the rotor plus a blunt capsule may offer weight savings over the more slender lifting-body-type entry vehicles because of higher volume-to-weight ratio and the simplicity of attaching a booster. Using a rotor to recover space vehicles is not a new idea and has been the subject of numerous theoretical investigations.[1–7]

In a recoverable space vehicle a certain portion of the total weight is made necessary by the recovery operation. This weight varies with the recovery technique and can run as high as 15% of the total recovered weight. It was reasoned that if the rotor with its accompanying weight penalty were acceptable because of its low-speed flight and landing characteristics, then the next logical step would be to examine what other benefits might be derived from the rotor. The most significant of these reported are that the rotor can provide improved vehicle stability, a greater range, and variable aerodynamic characteristics with little or no change in vehicle attitude.

Previous investigators have experimentally studied various aspects of vehicle recovery by rotors. Low-speed experimental results of unpowered rotors for space vehicle recovery have been examined by Hodson,[8] and Barzda and Schultz[9] using a radio-controlled free-flight model investigated the behavior of rotors for recovery applications. Supersonic tests of a rotor in near axial flight were reported by Galigher.[10]

If the rotor is to provide lift for maneuvering, it should be flown at low angles of attack as in gliding (rather than axial flight), where maximum lift-drag ratio provides substantial gains in range control and increases the decision time during the landing approach. At these low angles of attack, there has been no experimental information concerning vehicle trim, useful lift-drag ratio, and control power requirements. The present study concerns the experimental determination of the aerodynamic and operating characteristics of a rotor entry vehicle. The study was performed to assess the feasibility of using an unpowered lifting rotor at high forward speeds. The test results summarized herein are believed to be the first such results obtained on an unpowered rotor at supersonic speeds at glide attitude.

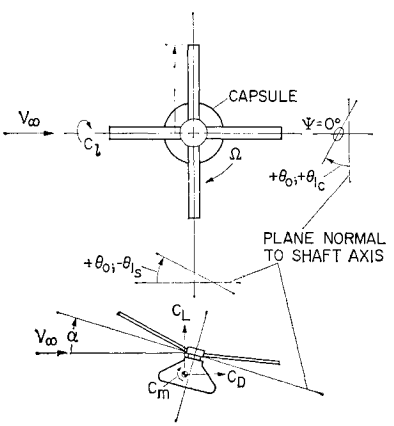

Fig. 1 Force and angle definition.

Presented as Paper 68-950 at the AIAA 2nd Aerodynamic Deceleration Systems Conference, El Centro, Calif., September 23–25, 1968; submitted November 6, 1968.

* Research Scientist.
† Research Scientist. Member AIAA.

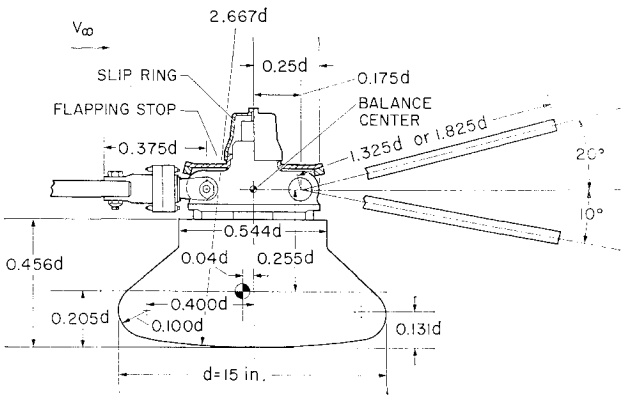

a) Geometry

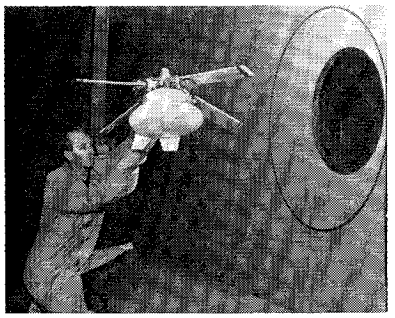

b) Model in low angle configuration with flaps deflected 180°

Fig. 2 Rotor entry vehicle wind-tunnel model.

Model Description and Instrumentation

The force and angle definitions are shown in Fig. 1 and the model geometry is presented in Fig. 2. The rotor entry vehicle model tested is a four-bladed rotor mounted on a capsule forebody. The mechanical design and fabrication were performed by the Kaman Corporation according to general specifications provided by Ames Research Center. Figure 2a is a drawing of the model. Figure 2b shows the model with flaps deflected 180°.

Rotor

The rotor has both collective and cyclic pitch degrees of articulation. The rotor was free to flap about offset flapping hinges. Both the collective and cyclic pitch could be changed remotely, either independently or in combination, through a conventional swash plate. The range of collective pitch travel available through use of the remote control system is ±20°. Both the lateral and longitudinal cyclic pitch have a range of ±10°. The design operating tip speed is 1100 fps. A detailed description of the model, control system features, and strength requirements is noted by Hollrock.[11]

Blades

The rotor blades were fabricated of a fiberglass epoxy laminate with most of the fibers oriented in the radial direction, giving the blades an extremely high strength-to-weight ratio in the radial direction. The blade airfoil section tested was a modified elliptical section (Fig. 3). The maximum thickness-to-chord ratio is 20%. The rotor blades are untwisted and have a rectangular planform. Two blade lengths were tested; the rotor diameters of 45 and 60 in. corresponded to rotor solidities of 20 and 15%, respectively. Aerodynamic heating governed the selection of the blade airfoil section, which, although not an efficient shape for supersonic speeds, provides the geometry needed to minimize the aerodynamic heating at hypersonic speeds.

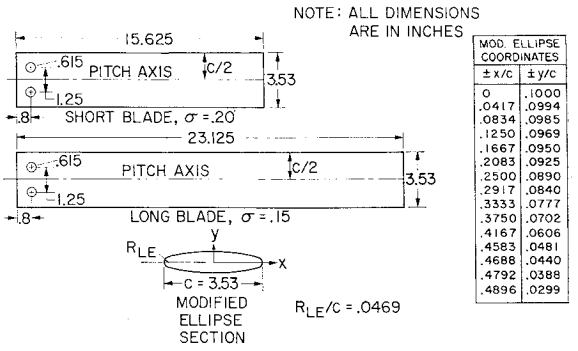

Fig. 3 Rotor entry vehicle blade geometry.

Body

The capsule was an aluminum body of revolution (Fig. 2). Its maximum diameter is 15 in., which gives a rotor-to-capsule diameter ratio of 3 and 4.

Model Mounting Details

In order to cover the 15° to 90° angle-of-attack range, three different model mounting arrangements were utilized (Fig. 4). In all cases the balance centerline was coincident with the rotor rotational axis with the electrical center of the balance coincident with the hub center. For the range 15° to 28°, the model and balance were mounted on a 90° elbow. In the 32° to 60° range the model and balance were mounted on a 30° bent adapter, attached to the model support strut. In the 62° to 90° range the model and balance were mounted in line with the sting. For the 32° to 90° range the wind-tunnel support system necessitated mounting the model upside down; hence the model lift was positive in the downward direction. (The rotor blades were very light so the moment of their weight, when mounted in this manner, was not significant.)

Instrumentation

The model forces were measured by means of a six-component internal strain-gage balance. The readout instrumentation consisted of indicating millivolt potentiometers. Rotor rpm was obtained from a magnetic pickup mounted on the stationary swash plate inside the model. The rotating part of the wash plate had 60 teeth around the circumference. The pulses generated as the teeth passed the magnetic pickup were measured electrically by a counter to determine rotor rpm.

Test Procedure

In the axial flow tests ($\alpha = 90°$), the blades were folded back along the sting before the wind tunnel was started.

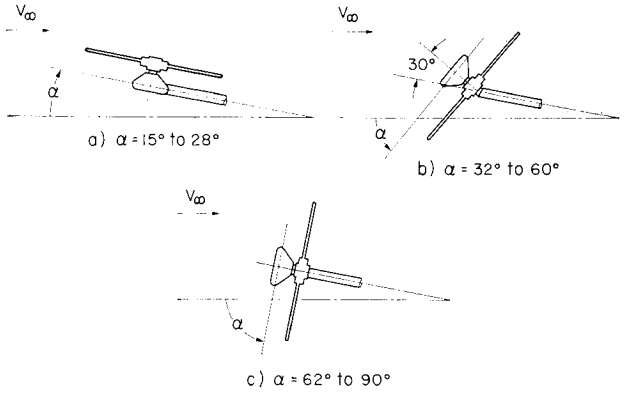

Fig. 4 Model mounting arrangements.

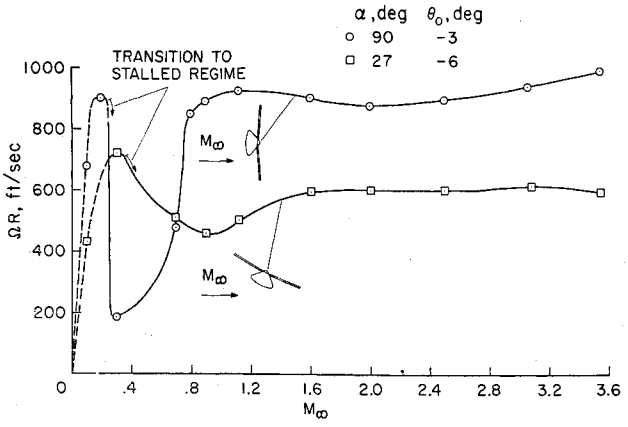

Fig. 5 Variation of autorotative equilibrium rotor speed with freestream Mach number.

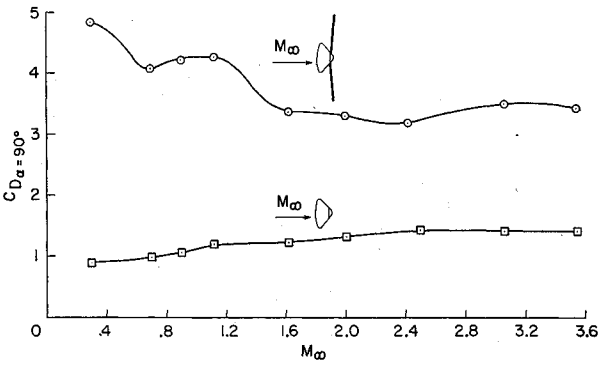

Fig. 7 Effect of Mach number on the drag coefficient in axial flight.

(For tests in this attitude the flapping stop, shown in Fig. 2, was removed from the hub.) When the tunnel reached test conditions both collective and cyclic pitch were used to deploy the rotor as in the recovery process. Before the tunnel was shut down, the rotor was stopped by setting the blade pitch to zero. Under these conditions the flow holds the blades back along the sting. This procedure was utilized to minimize possible damage to the rotor during the tunnel shutdown operations. At low and intermediate angles of attack, rotor rotation was initiated at a freestream dynamic pressure of about 50 psf by use of the collective pitch control.

The investigation was conducted by parametrically varying the blade pitch angle at fixed conditions of freestream Mach number and angle of attack. During the test operations only collective pitch and either "longitudinal" (sine component of blade feathering) or "lateral" (cosine component of blade feathering) cyclic pitch was used. No tests were made which utilized both cyclic pitch controls simultaneously. When cyclic pitch was employed, it was varied at a fixed value of collective pitch angle.

Results and Discussion

The results of the experimental investigation of the operating and aerodynamic characteristics of a rotor entry vehicle model are presented in Figs. 5 through 15. All data are for the 45-in.-diam rotor except for Fig. 12, which has data for both rotor diameters.

Operating Characteristics

The variations of autorotative equilibrium tip speed with freestream Mach number are shown in Fig. 5. Curves are presented for two angles of attack and 0° of cyclic pitch.

In axial flight ($\alpha = 90°$) the rotor speed increases rapidly between $M_\infty = 0.1$ and 0.2 because of the increase in freestream velocity. This range, in which the blades are operating primarily in an unstalled flow, is denoted by the dashed portion of the curve. Because the blades have no twist, some of the blade sections are stalled. Operation in this speed range corresponds to the classical windmill condition for an unpowered rotor. Transition to a fully stalled flow regime between $M_\infty = 0.2$ and 0.3 occurs with an accompanying rapid decrease in rotor speed. As the Mach number is increased beyond 0.3, the rotor speed increases rapidly until $M_\infty = 0.8$. Further increases in Mach number have only a slight effect on the rotor speed. At $\alpha = 27°$ there is an increase in rotor speed as the Mach number increases from 0.1 to 0.3. This is a result of the increase in freestream velocity and corresponds to the classical autorotation regime. From $M_\infty = 0.3$ to 0.9 there is a decrease in rotor speed as the rotor enters the fully stalled regime. Above $M_\infty = 0.9$ the rotor speed increases until $M_\infty = 1.6$ is reached and then remains essentially constant to $M_\infty = 3.54$.

The variations in rotor speed with Mach number discussed in the preceding paragraphs were for particular blade pitch angles. One of the problems associated with autorotating rotor systems is that at low forward speeds the variation of rotor speed with blade pitch angle can become unstable. This is shown in Fig. 6, where typical variations of dimensionless tip speed as a function of blade pitch angle for various subsonic Mach numbers are presented. These data are for an angle of attack of 20°. Note that instability in rotor speed occurs at this angle of attack at $M_\infty = 0.2$ and below. As the Mach number is increased from 0.1 to 0.2, the instability moves from the positive blade pitch angle range to the negative blade pitch range. At $M_\infty = 0.3$ the rotor speed instability has disappeared completely. Although not shown, data for other angles of attack investigated indicate that at $M_\infty = 0.3$ and above, the variation of rotor speed with blade pitch angle is stable. Increasing the Mach number above 0.3 reduces the initial rapid rise in tip speed ratio at low collective pitch angles. At $M_\infty = 0.7$ the variation of tip speed with collective pitch angle has become relatively flat.

Rotor speed instability occurs when the blade alternately becomes stalled and unstalled, resulting in multiple rotor

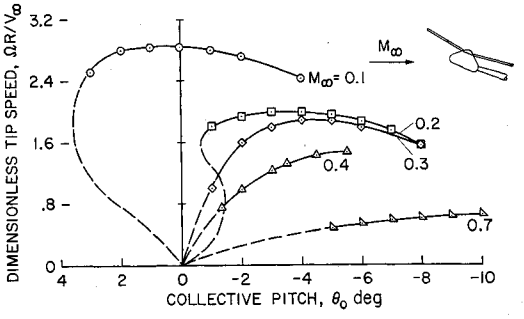

Fig. 6 Variation of equilibrium autorotative tip speed ratio with blade pitch angle; $\alpha = 20°$.

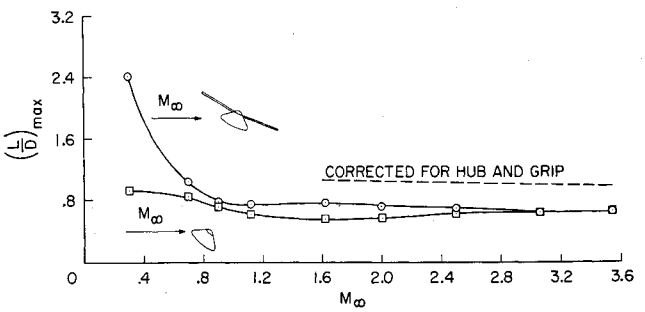

Fig. 8 Effect of Mach number on the maximum lift-drag ratio.

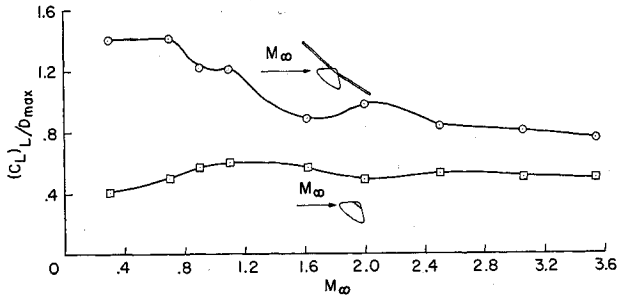

Fig. 9 Lift coefficient for maximum lift-drag ratio.

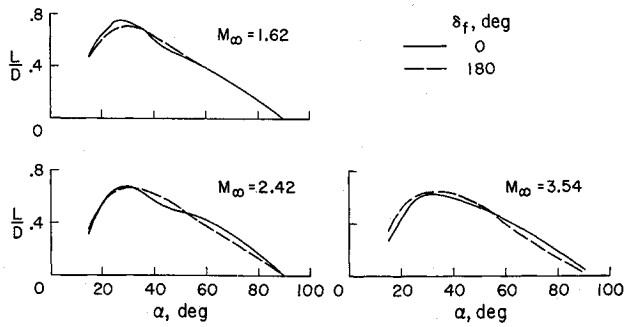

Fig. 11 Effect of flap deflection on the lift-drag ratio.

speeds for the same blade pitch angle. Hence, it is not known at which rotational speed the rotor will operate if this flow condition occurs. Tests at supersonic speeds[10] indicated no instabilities in axial flight, but similar results for low angles of attack were not available. Theoretical studies[1,5] indicated that there should be no instabilities at supersonic speeds, but the theory was invalid for unstalled operation and hence could not predict when rotor speed instability would occur as the Mach number was reduced below 1.

Aerodynamic Characteristics

Drag

The drag coefficient of the rotor vehicle compared with that of the capsule alone for an angle of attack of 90° (attitude for maximum braking) is shown in Fig. 7. The addition of the rotor provides a substantial increase in the drag coefficient. The drag of the complete vehicle is about five times the drag of the capsule alone at $M_\infty = 0.3$, decreasing to about 2.3 times at $M_\infty = 3.54$. Theoretical studies[1] have shown that this increase in drag coefficient results in essentially the same maximum deceleration g as the capsule alone. However, the altitude at which the speed becomes subsonic is nearly doubled, being in excess of 100,000 ft. It is obvious that the higher the altitude at which subsonic flight can be reached, the greater the maneuvering capability and time available for landing site selection and final-approach flight-path adjustments.

Lift-drag ratio

The variation of maximum lift-drag ratio with Mach number is shown in Fig. 8. The corresponding lift coefficient at maximum L/D is shown in Fig. 9. At Mach numbers below 0.7 the addition of a rotor to the capsule provides substantial gains in $(L/D)_{max}$. At $M_\infty = 0.3$ the combined $(L/D)_{max}$ is nearly three times as great as for the capsule alone. At Mach numbers 0.7 and above, the advance ratio ($V_\infty \cos\alpha/\Omega R$) was greater than 1.0. It should be noted that for the wind-tunnel model tested, the hub and blade grip mechanism is too large in proportion to the capsule (Fig. 2). This was necessitated by the large factor of safety requirements for tests conducted in the Ames wind-tunnel facilities, and is a common problem of scaling rotors. Consequently, the drag due to the hub and blade grips is much higher than would be expected on a full-scale system. Recent results obtained to assess the drag due to the grips and hub indicate that at supersonic speeds the maximum lift-drag ratio of a vehicle with a properly proportioned hub is slightly more than 1.0.

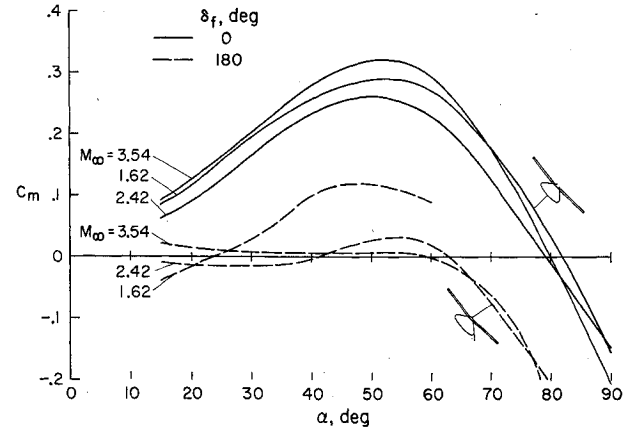

Fig. 10 Effect of flap deflection on the pitching moment of a rotor entry vehicle.

Pitching moment

The pitching moment as a function of angle of attack for three supersonic Mach numbers is shown in Fig. 10. These moments were too large, in most instances, to be trimmed by the cyclic pitch controls; hence, flaps were installed on the capsule. Tests were conducted at flap settings of 0° and at the maximum deflection angle of 180°. With no flap deflection the vehicle is unstable at angles of attack from 15° to about 50°. Deflecting the flaps to 180° position indicates that essentially neutral stability can be obtained over a large angle of attack range at $M_\infty = 2.42$ and 3.54. At $M_\infty = 1.62$ the vehicle is still unstable at low to moderate angles of attack, but the level of the pitching-moment coefficient has been markedly reduced. At angles of attack near maximum L/D, the vehicle can be trimmed by use of the cyclic pitch controls.

Effect of flaps on L/D

The effect of flap deflection on the lift-drag ratio is shown in Fig. 11. The left-drag ratio is presented as a function of angle of attack for the three supersonic Mach numbers shown in Fig. 10. Generally, deflecting the flaps has little effect on the lift-drag ratio. Although drag data with and without flaps are not presented, tests indicated that the flaps increased the drag coefficient by 2% in the glide attitude.

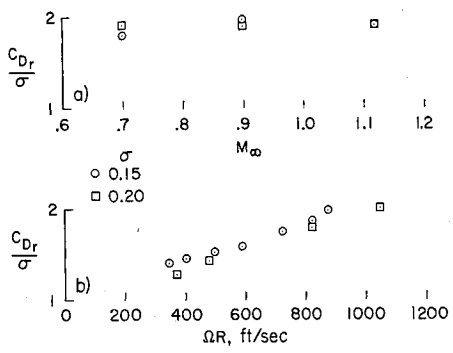

Fig. 12 Effect of rotor solidity on the rotor drag coefficient; $\alpha = 90°$. a) $\Omega R = 830$ fps; b) $M_\infty = 0.9$.

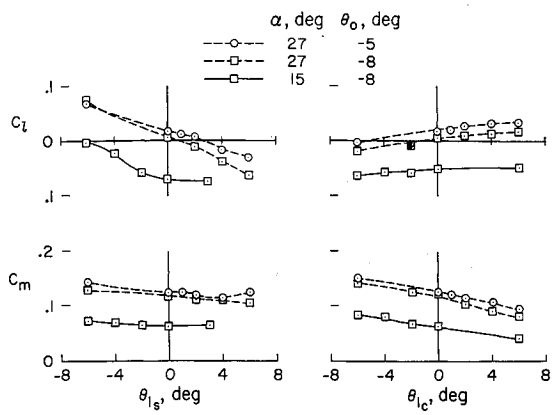

Fig. 13 Vehicle trim characteristics; $M_\infty = 2.5$.

Rotor solidity effects

Values of the rotor drag coefficient with four short blades ($\sigma = 0.20$) and four long blades ($\sigma = 0.15$) are presented in Fig. 12. The variation of rotor drag coefficient at transonic speeds is shown in Fig. 12a for a tip speed of 830 fps. The comparison at $M_\infty = 0.9$ with rotor tip speed as the variable is shown in Fig. 12b. The long blades have the same airfoil cross section as the short blades, but their length results in a rotor diameter of 60 in. The drag coefficients shown are based on freestream dynamic pressure and rotor disk area at 0° flapping angle. The data presented were obtained by subtracting the capsule alone drag from the combined rotor-capsule drag. No corrections for interference of the capsule flowfield on the rotor have been taken into account. The close correspondence for the two rotors indicates that the rotor drag coefficient is directly proportional to solidity as indicated by theory.[1,5]

Trim control characteristics

The rotor trim characteristics resulting from use of the cyclic pitch controls are presented in Figs. 13–15. It should be pointed out again that these controls were varied parametrically, as discussed in the section entitled "Test Procedure." The rolling- and pitching-moment coefficients as functions of longitudinal and lateral cyclic pitch angle are shown for $M_\infty = 2.5$ in Fig. 13. Data are presented for two angles of attack in the glide attitude and in one case for two values of the blade collective pitch angle. The use of longitudinal cyclic pitch (Θ_{1s}) has little effect on the pitching moment but provides considerable roll control power. This effect is opposite to the expected response of an ideal rotor and represents a large change in the control phasing. Use of the lateral cyclic pitch control (Θ_{1c}) has a slightly greater effect on the pitch control power than on the roll control power. The amount of pitch control power available through use of lateral cyclic pitch is sufficient to trim the vehicle when used in conjunction with a pitch flap deflection of 180°.

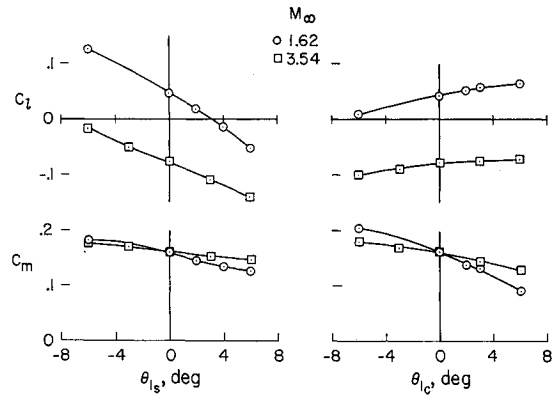

Fig. 14 Variation of vehicle trim characteristics; $\alpha = 27°$, $\theta_0 = -8°$.

Variations in rolling and pitching moment with cyclic pitch angle for other Mach numbers are presented in Fig. 14. These data are for an angle of attack of 27° and collective pitch angle of −8°. Data are presented for Mach numbers 1.62 and 3.54. The effects of cyclic pitch control are the same as discussed in the preceding paragraph. The effect of Mach number is generally negligible on both the pitch and roll control power. However, there is a large change in roll trim with increasing Mach number.

The pitch and roll control power characteristics as a function of Mach number are shown in Fig. 15. The derivatives presented are for an angle of attack of 27° and a collective pitch angle of −8°. The derivatives shown were evaluated at 0° cyclic pitch. Generally, Mach number has only a small effect on both the pitch and roll control power for Mach numbers between 0.7 and 3.54. The roll control power is greatest when longitudinal cyclic pitch is used (Fig. 15a). In absolute magnitude, longitudinal cyclic pitch produces about three times the roll control power that is produced by the lateral cyclic pitch control for Mach numbers up to about 2.0. Above $M_\infty = 2.0$ longitudinal cyclic pitch has about five times as much roll control power as the lateral cyclic pitch. The use of either cyclic pitch control produces about the same pitch control power for Mach numbers 2.0 and higher (Fig. 15b). Between Mach numbers 1.2 and 2.0, lateral cyclic pitch must be used to obtain the greatest amount of pitch control power. Comparison for a given cyclic pitch control indicates that the most significant effect is that there is a large change in the control phasing when the longitudinal cyclic pitch control is used. This may be due, in part, to the large flapping offset ($\simeq$12%). However, simplified theories for a rotor with flapping hinge offsets do not predict a phase shift of the experimentally obtained magnitude.

Concluding Remarks

An experimental investigation has been made to examine the characteristics of an unpowered rotor entry vehicle at speeds up to $M_\infty = 3.54$. The results obtained for the operating and aerodynamic characteristics of an unpowered rotor appear to make the system well suited for recovery of space vehicles. The test results indicate that at $M_\infty = 0.3$ and higher the rotor speed is stable at all blade pitch angles and angle of attack. The rotor speed instabilities due to partial stall operation in normal low-speed helicopter operation do not appear at high Mach numbers. Substantial increases in drag can be obtained for entry vehicle braking. It was found that the rotor drag coefficient was proportional

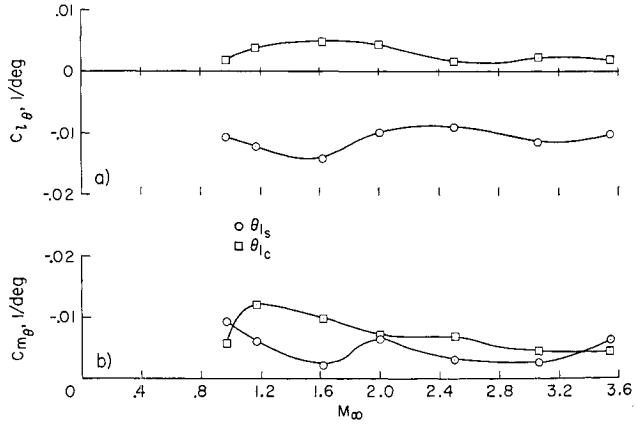

Fig. 15 Mach number effect on the pitch- and roll-control power characteristics; $\alpha = 27°$, $\theta_0 = -8°$. a) Roll-control power; b) pitch-control power.

to rotor solidity as indicated by theory. Low-speed lift-drag ratio can be greatly improved by adding a rotor to a conical lifting capsule. At supersonic speeds the rotor contributes only slightly to the capsule-alone lift-drag ratio. In order to trim the vehicle at supersonic speeds, a combination of flap deflection and cyclic pitch control must be used. Deflecting the flaps results in nearly neutral stability over a large portion of the angle-of-attack range with negligible effect on the lift-drag ratio. The effectiveness of the cyclic pitch control for roll and pitch control was found to be generally insensitive to Mach number at low angles of attack. The most noticeable effect regarding the use of the cyclic pitch controls was the large control phasing when longitudinal cyclic pitch was used. The pitch control power was about the same when either longitudinal or lateral cyclic pitch was used, except between Mach number 1.2 and 2.0, where lateral cyclic pitch produced the greatest pitch control power.

References

[1] Levin, A. D. and Smith, R. C., "An Analytical Investigation of the Aerodynamic and Performance Characteristics of an Unpowered Rotor Entry Vehicle," TN D-4537 1968, NASA.

[2] Kretz, M., "Application of Rotary Wing Techniques to Atmospheric Re-entry and Launch Vehicle Recovery Problems," presented at European Symposium on Space Technology, June 1961, London.

[3] Haig, C. R., Jr., "The Use of Rotor for the Landing and Re-entry Braking of Manned Spacecraft," Paper 60-17, 1960, IAS.

[4] Barzda, J. J., "Investigation of Stored Energy Rotors for Recovery," TDR-63-745, Dec. 1963, Aeronautical Systems Div. U.S. Air Force.

[5] Ham, N. D., "An Experimental and Theoretical Investigation of a Supersonic Rotating Decelerator," *Journal of the American Helicopter Society*, Jan. 1963.

[6] Haig, C. R., Jr., "Aerodynamic Analysis of a Rotor in the Fully Stalled Propeller Braking State," Rept. 8008-099-003, March 1960, Bell Helicopter Co., Fort Worth, Texas.

[7] Haig, C. R., Jr., "An Aerodynamic Analysis of a Lifting Rotor in Hypersonic Flight," Rept. 8008-099-001, June 1959, Bell Helicopter Co., Fort Worth, Texas.

[8] Hodson, J. S., "Low Speed Wind Tunnel Test of 12-Foot and 14-Foot Diameter Rotochutes," Rept. 7-93, Jan. 1957, Kaman Aircraft Corp., Bloomfield, Conn.

[9] Barzda, J. J. and Schultz, E. R., "Test Results of Rotary-Wing Decelerator Feasibility Studies for Capsule Recovery Applications," Paper 756D, Sept. 1963, Society of Automotive Engineers, New York.

[10] Galiger, L. L., "Wind Tunnel Tests of the Kaman KRC-6M Rotochute at Supersonic Speeds," TDR-63-128, July 1963, Arnold Engineering Development Center.

[11] Hollrock, R., "Final Report, Rotor Entry Vehicle Wind Tunnel Model," Rept. R-581, May 1965, Kaman Aircraft Corp., Bloomfield, Conn.